Time-sequential pipelined imaging with wavefront coding and super resolution.

Laura. V. Cowan, Paul Zammit, Guillem Carles, Andrew. R. Harvey
School of Physics & Astronomy, Kelvin Building, University of Glasgow, Glasgow, G12 8QQ United Kingdom.
l.cowan.1@research.gla.ac.uk

Abstract: Wavefront coding has long offered the prospect of mitigating optical aberrations and extended depth of field, but image quality and noise performance are inevitably reduced. We report on progress in the use of agile encoding and pipelined fusion of image sequences to recover image quality.
OCIS codes: (100.3020) Image reconstruction-restoration; (100.6640) Superresolution; (110.1758) Computational imaging, (100.0100) Image processing, (110.7348) Wavefront encoding, (110.6820) Thermal imaging, (110.6915) Time imaging.

The seminal paper by Dowski and Cathey describing the extension of depth of field by wavefront coding [1] marked the dawning of the field of computational imaging. Extended depth of field is achieved by optical coding using a refractive phase mask to yield an approximately defocus-invariant point-spread function (PSF) combined with digital decoding. The resultant insensitivity to defocus and higher-order optical aberrations has enabled applications ranging from high-performance wide field-of-view thermal imaging using a wavefront coded singlet [2], to extended depth of field 3D-ranging microscopy [3]. The encoding of the PSF is associated with a suppression of the modulation-transfer function (MTF) and strong phase modulations in the optical-transfer function (OTF) that result in signal-to-noise ratio (SNR) degradation and artefacts in the recovered images. The highest quality of image recovery, in the sense that the Mean Structural Similarity (MSSIM) is highest, is generally obtained not by the cubic mask proposed in [1], but by the generalised cubic function, or trefoil phase function [4,5], given by,

$$q(x,y) = \alpha(x^3 + y^3) - 3\alpha(x^2y + xy^2) \qquad (1)$$

where x and y are normalised pupil coordinates and α characterises the amplitude of the phase-modulation. The associated trade-off between image quality and insensitivity to optical aberrations means that optimal implementation of wavefront coding involves sparing use of wavefront coding; the amplitude, α, of wavefront coding introduced should be the minimum that enables optical aberrations to be mitigated. Previous research has addressed the problem of increased noise in wavefront-coded systems [6]. We report here three further measures to mitigate the inevitable reduction in SNR associated with wavefront coding: (1) variable wavefront coding, (2) pipelined fusing of video sequences to enhance SNR and (3) time-sequential super-resolution imaging of video sequences.

An advantage of the generalised cubic phase mask is that by combining two masks with a mutual rotation θ, the resultant amplitude of coding, α, varies continually between zero and a maximum value as θ varies between 0 and 60°, as can be appreciated by the masks depicted in the top row of Figure 1. This yields a point-spread function that varies between a diffraction-limited spot and an extended PSF as shown in the lower row for θ = 0°, 30° and 60°. The former yields the highest SNR and smallest depth of field while the latter yields the greatest depth of field and maximum suppression of SNR; an agile trade of SNR vs depth of field is possible by a simple rotation of the phase mask.

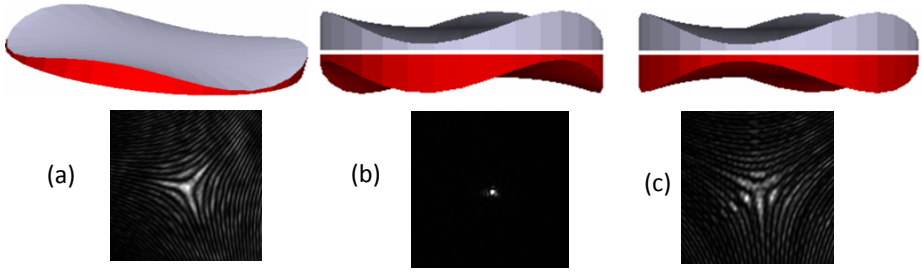

Figure. 1. Point spread functions experimentally recorded by rotation of one of two petal phase masks by (a) 0º, (b) 30º, and (c) 60º from the position in Fig. 1(b).

For a given degree of wavefront coding, suppression of SNR is inevitable, but there is scope for recovery of SNR by exploitation of redundant information within image sequences. It is this redundancy that forms the basis of the efficient low-loss data compression that is possible with MPEG video compression. Here we use it to conduct pipelined fusing of images within a video sequence to generate an output video sequence in which boxcar integration is applied to the areas of images not subject to change; that is, image areas where the

transformation between images is an affine transform. Co-registered, averaged, and segmented image areas between which there is significant change are not averaged. In this way, there is an agile, real-time trade of SNR against time resolution that varies across the image and across the video sequence: in image areas where time resolution is not required, it is sacrificed in favour of SNR. Generally, when the imager is handheld there is randomised motion between the imager and the scene, requiring frame-to-frame co-registration. In addition, this movement will tend to randomise the sampling phase of the scene by the detector array thus enabling a high-quality super-resolution image to be computed from the video frame sequence [7-9].

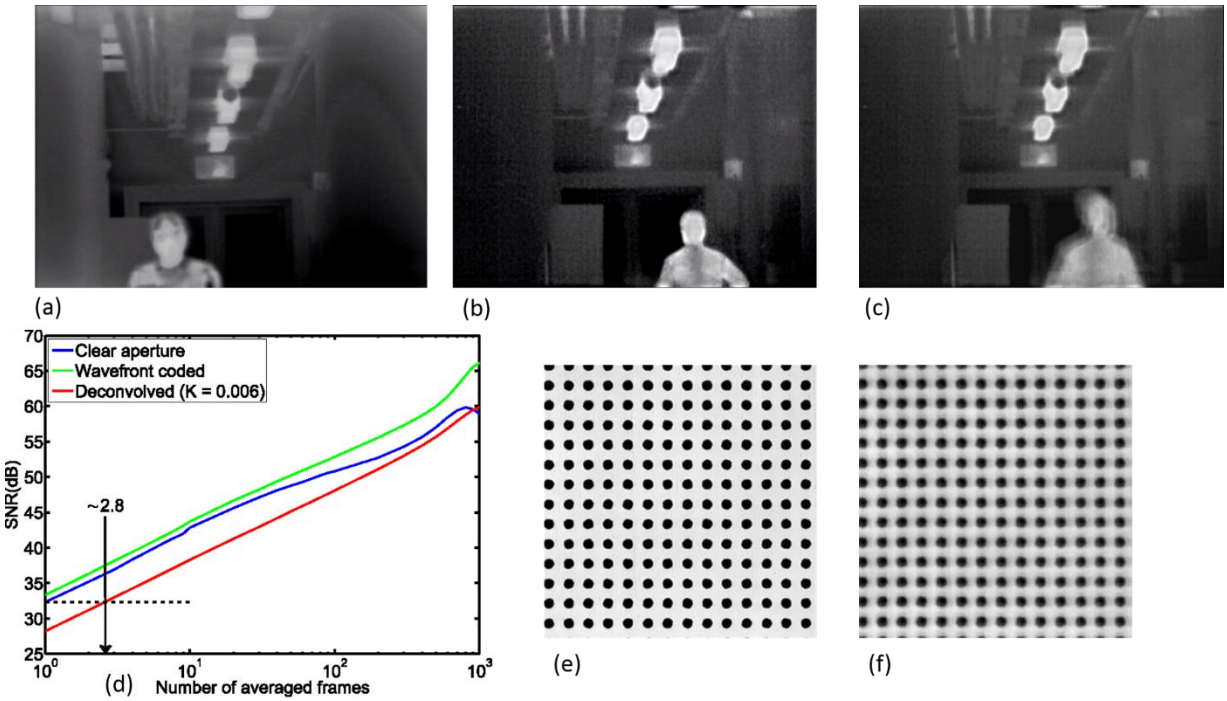

Figure 2: (a) Long Wave Infrared (LWIR) video frame; (b) a LWIR wavefront coded video frame; (c) a LWIR wavefront coded video frame combined with pipelined fusing of images. (d) Improvement in SNR against number of averaged frames obtained from micrographs of a distortion target imaged in transmission at 540 +/- 20nm. (e) and (f) diffraction limited and wavefront coded images of the distortion target respectively.

The video frames in figure 2 were recorded using a LWIR camera, figures 2(a), 2(b), and 2(c) are compared to show the gradual improvement of the wavefront coded images - 2(b) and (c) - to the initial image without a phase mask in the pupil plane. The extended depth of field can be seen in the wavefront coded images, however so can the image degradation due to the increased overall noise.

Figure 2 (c) has been processed with pipelined fusing of images and shows an objective enhancement in SNR, specifically in the background random noise of the images. In this image, time-sequential pipelined imaging introduces some artefacts in areas in which boxcar integration is applied. Figure 2 (c) shows artefacts surrounding the moving figure in a wavefront coded scene, due to imperfect segmentation of the moving components which will be reduced or eradicated by future research.

Figure 2(d) shows the improvement in SNR with the number of pipeline fused frames for the diffraction limited, wavefront coded, and the recovered wavefront coded images which have been deconvolved using a parametric Wiener filter (with a scalar noise-to-signal power ratio of K = 0.006). These were obtained from micrographs of a distortion target acquired using a 20x, 0.5NA objective in transmission and an illumination wavelength of 540 ± 20nm. The wavefront coded images were acquired using a cubic phase mask with an α of ~ 6λ. In each instance, 2500 images were taken of the scene, registered with respect to one another and ultimately averaged. This was then used as an estimate of the noise-free image, I_s. I_s for the diffraction limited and wavefront coded cases are shown in Figure 2(e) and (f) respectively. The noisy images for N averaged frames, I_{ns}^N ; where $N \in [10,1000]$, were then calculated by simply averaging N frames. The SNR was then calculated using the following definition:

$$\text{SNR} = 20\log_{10}(I_{max}/\delta_n), \tag{2}$$

where I_{max} is the maximum signal of I_s, and δ_n is the standard deviation of $(I_{ns}^N - I_s)$. In using this definition, we assume the peak signal is equivalent for the diffraction limited case and the wavefront coded case, however the recovered wavefront coded data inhabits the characteristic noise amplification of a wavefront coding system and is where the pipeline fusing improvement is most beneficial. Indicated on Figure 2 (d) is that fusing

~2.8 deconvolved wavefront coded frames together results in a noise power equivalent to a single diffraction limited frame for the given experimental setup.

From equation (2), the SNR is expected to increase at a rate of 10dB/decade. By fitting a straight line to the curves shown in Figure 2(d), the increase in SNR was found to be 8.9dB/decade, 10.3dB/decade and 10.4dB/decade for the diffraction limited case, wavefront coded case and recovered wavefront coded case respectively, which correlate well with the expected rate.

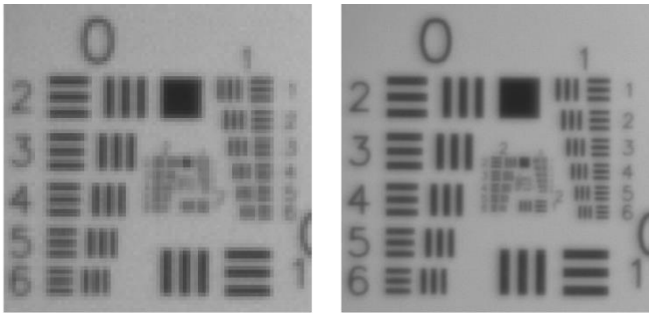

Figure 3 (a) a resolution-limited video frame of a USAF target taken with a visible handheld camera; (b) a frame from the same footage time-sequentially super-resolved.

As mentioned above, the possibility of exploiting the relative motion between the imager and scene enables pipelined super resolution of image sequences [7]. Figure 3 shows an example of time-sequential super resolution recorded using a visible-band handheld camera, with figure 3 (a) showing the pixel-limited image and figure 3(b) showing the time-sequentially super-resolved image. As expected, figure 3(b) shows a notable improvement from figure 3 (a) due to this post-processing step. The redundancy present in the pipelined fusing algorithm provides a platform to combine this technique with time-sequential super resolution. This will decrease the presence of artefacts in the system, such as in figure 2 (c), to a sufficient level to produce an output image more similar to that which can be recorded in a non-wavefront coded system - with less degradation of image quality.

In conclusion, we report on-going work in enhancing the image quality of wavefront-coded video sequences to simultaneously achieve a high image quality and access the benefits of aberration-tolerant imaging provided by wavefront coding; such as a wide field-of-view and the reduced size, weight, and cost of imaging optics. Preliminary experiments indicate the promise of SNR improvement and super-resolution enhancement by using a pipelined fusion of video sequences recorded with a phase mask based on the generalised cubic function. Future work will aim to improve the fusion and recovery of images, addressing two fundamental challenges: optimising SNR up to the maximal limit (by a factor equal to the square root of the number of averaged images) and high quality segmentation of changing and non-changing scene components.

References

[1] Dowski ER, Cathey WT. Extended depth of field through wave-front coding. Applied optics. 1995 Apr 10;34(11):1859-66.

[2] Muyo, G., & Harvey, A. (2004). Wavefront coding for athermalization of infrared imaging systems, 5612, 227–235.

[3] Zammit, P., Harvey, A. R., & Carles, G. (2014). Extended depth-of-field imaging and ranging in a snapshot. Optica, 1(4), 209–216. https://doi.org/10.1364/optica.1.000209

[4] Vettenburg T, Bustin N, Harvey AR. Fidelity optimization for aberration-tolerant hybrid imaging systems. Optics express. 2010 Apr 26;18(9):9220-8.

[5] Prasad, S., Torgersen, T., Pauca, V., Plemmons, R., & van der Gracht, J. (2003). Engineering the pupil phase to improve image quality. Proc. SPIE, 5108, 1–12.

[6] S. Bradburn, W. T. Cathey, and E. R. Dowski, "Realizations of focus invariance in optical–digital systems with wave-front coding," Appl. Opt., vol. 36, no. 35, pp. 9157–9166, 1997.

[7] Young, S. S., & Driggers, R. G. (n.d.). Superresolution image reconstruction from a sequence of aliased imagery.

[8] Downing, J., Findlay, E., Muyo, G., & Harvey, A. R. (2012). Multichanneled finite-conjugate imaging. Journal of the Optical Society of America A, 29(6), 921.

[9] Carles, G., Downing, J., & Harvey, A. R. (2014). Super-resolution imaging using a camera array. Optics Letters, 39(7), 1889.